

# Characterization of the activity, aggregation, and toxicity of heterodimers of WT and ALS-associated mutant Sod1

Aline de Araújo Brasil<sup>a,1</sup>, Mariana Dias Castela de Carvalho<sup>a,1</sup>, Ellen Gerhardt<sup>b,c,d</sup>, Daniela Dias Queiroz<sup>a</sup>, Marcos Dias Pereira<sup>a</sup>, Tiago Fleming Outeiro<sup>b,c,d,e,f,2</sup>, and Elis Cristina Araujo Eleutherio<sup>a,2,3</sup>

<sup>a</sup>Institute of Chemistry, Federal University of Rio de Janeiro, 21941-909 Rio de Janeiro, RJ, Brazil; <sup>b</sup>Department of Experimental Neurodegeneration, University Medical Center Göttingen, 37073 Göttingen, Germany; <sup>c</sup>Center for Nanoscale Microscopy and Molecular Physiology of the Brain, University Medical Center Göttingen, 37073 Göttingen, Germany; <sup>d</sup>Center for Biostructural Imaging of Neurodegeneration, University Medical Center Göttingen, 37073 Göttingen, Germany; <sup>e</sup>Max Planck Institute for Experimental Medicine, 37075 Göttingen, Germany; and <sup>f</sup>Institute of Neuroscience, Newcastle University Medical School, NE2 4HH Newcastle Upon Tyne, United Kingdom

Edited by Gregory A. Petsko, Brigham and Women's Hospital, New York, NY, and approved November 4, 2019 (received for review February 11, 2019)

**Mutations in Cu/Zn superoxide dismutase (Sod1) have been reported in both familial and sporadic amyotrophic lateral sclerosis (ALS). In this study, we investigated the behavior of heteromeric combinations of wild-type (WT) and mutant Sod1 proteins A4V, L38V, G93A, and G93C in human cells. We showed that both WT and mutant Sod1 formed dimers and oligomers, but only mutant Sod1 accumulated in intracellular inclusions. Coexpression of WT and hSod1 mutants resulted in the formation of a larger number of intracellular inclusions per cell than that observed in cells coexpressing WT or mutant hSod1. The number of inclusions was greater in cells expressing A4V hSod1. To eliminate the contribution of endogenous Sod1, and better evaluate the effect of ALS-associated mutant Sod1 expression, we expressed human Sod1 WT and mutants in human cells knocked down for endogenous Sod1 (Sod1-KD), and in *sod1Δ* yeast cells. Using Sod1-KD cells we found that the WT–A4V heteromers formed higher molecular weight species compared with A4V and WT homomers. Using the yeast model, in conditions of chronological aging, we concluded that cells expressing Sod1 heterodimers showed decreased antioxidant activity, increased oxidative damage, reduced longevity, and oxidative stress-induced mutant Sod1 aggregation. In addition, we also found that ALS-associated Sod1 mutations reduced nuclear localization and, consequently, impaired the antioxidant response, suggesting this change in localization may contribute to disease in familial ALS. Overall, our study provides insight into the molecular underpinnings of ALS and may open avenues for the design of future therapeutic strategies.**

Sod1 | amyotrophic lateral sclerosis | aging | heterodimers

**A**myotrophic lateral sclerosis (ALS) is a progressive and devastating neurological disease characterized by the loss of motor neurons in the spinal cord, motor cortex, and brainstem (1). The prevalence of ALS is ~4 to 7 per 100,000. The etiology is complex and can present as sporadic (sALS) (90 to 95% of cases), or familial (fALS) (5 to 10% of cases) (1–3). However, several gene mutations have been observed in patients with either familial or sporadic forms of ALS.

Among the fALS cases, 20 to 25% are associated with mutations in the Cu/Zn isoform of superoxide dismutase (Sod1), encoded by the *SOD1* gene. Sod1 is widely distributed throughout the cell, including in the cytoplasm, lysosomes, and the intermembrane space of mitochondria. More recently, it was also detected in the nucleus, as a response to oxidative stress (4, 5). Sod1 is responsible for the dismutation of superoxide anions and, in recent studies, it was associated with the expression of antioxidant and repair genes (5). Indeed, fALS-associated Sod1 mutations were initially thought to lead to a loss of dismutase function (6, 7). However, a toxic gain of Sod1 function may also contribute to disease, since *SOD1* knockout animals do not exhibit ALS-like phenotypes (4). Importantly, fALS

is primarily a heterozygous genetic condition and over 150 mutations have been identified in human Sod1 (hSod1) (8). Nevertheless, despite extensive research, the underlying causes of ALS and the paths of neurodegeneration remain elusive.

We recently showed that expression of fALS hSod1 mutant (A4V, L38V, G93A, and G93C) homodimers results in increased hSod1 aggregation, in intracellular oxidation, and in genomic instability due to the hSod1 mislocalization, when compared to the expression of WT hSod1 (9). Several studies showed that coexpression of human WT and mutant Sod1 accelerates disease in transgenic animals (10–12). In this context, it has been proposed that WT Sod1 (human or mouse) may slow mutant Sod1 aggregation (13, 14). In addition, the formation of WT and mutant heterodimers might modulate Sod1 aggregation, which seems to be stabilized by the presence of WT protein (15, 16). Although most fALS studies have focused on the investigation of Sod1 homodimers/homomers, the investigation of Sod1 heterodimers/heteromers remains controversial, and poorly explored. Altogether our study provides insight into the molecular effects of both Sod1

## Significance

**Aggregation of the antioxidant enzyme Sod1 represents common factors of both familial (fALS) and sporadic cases of ALS, a fatal neurodegenerative disease. Although many ALS studies have focused on Sod1 homodimers/homomers, the investigation of Sod1 heterodimers/heteromers remains controversial and has mostly been performed with recombinant proteins in vitro, in the absence of a cellular environment. By using living cells, this study sheds light into a critical issue in the context of fALS, the high toxicity of the WT–mutant heteromeric inclusions, especially WT–A4V heteromers which accumulate both in human cells as well as in chronologically aged yeast cells. Besides the aggregation, we proposed that an inefficient heteromer response against oxidative conditions might contribute to fALS-linked mutant hSod1 toxicity.**

Author contributions: A.d.A.B., T.F.O., and E.C.A.E. designed research; A.d.A.B., M.D.C.d.C., E.G., and D.D.Q. performed research; A.d.A.B., M.D.C.d.C., E.G., M.D.P., T.F.O., and E.C.A.E. analyzed data; and A.d.A.B. and M.D.C.d.C. wrote the paper.

The authors declare no competing interest.

This article is a PNAS Direct Submission.

This open access article is distributed under [Creative Commons Attribution-NonCommercial-NoDerivatives License 4.0 \(CC BY-NC-ND\)](https://creativecommons.org/licenses/by-nc-nd/4.0/).

<sup>1</sup>A.d.A.B. and M.D.C.d.C. contributed equally to this work.

<sup>2</sup>T.F.O. and E.C.A.E. contributed equally to this work.

<sup>3</sup>To whom correspondence may be addressed. Email: [eliscael@iq.ufrj.br](mailto:eliscael@iq.ufrj.br).

This article contains supporting information online at <https://www.pnas.org/lookup/suppl/doi:10.1073/pnas.1902483116/-DCSupplemental>.

First published December 3, 2019.

homo- and heterodimers, establishing the basis for future studies that may impact on our understanding of the molecular underpinnings of ALS.

### Results

**Coaggregation of WT and fALS-Associated Mutant hSod1 Heterodimers in Human Cells.** In order to assess the aggregation of WT and mutant human Sod1 heteromers, we used the bimolecular fluorescence complementation (BiFC) assay (9, 17). In this assay, fluorescence requires the interaction between at least 2 proteins, each of which is fused to nonfluorescent, truncated fragments of a

fluorescent protein (e.g., Venus fluorescent protein) (Fig. 1A). Thus, the BiFC assay enables the study of homo- or heterodimeric protein species, which may then assemble into higher order oligomers (homomers or heteromers). We found that all heteromeric WT hSod1 and mutant hSod1 combinations formed dimers/oligomers and inclusions (Fig. 1B and C). In cells expressing WT hSod1 BiFC pairs, no inclusions were detected (Fig. 1C). Although the inclusions formed by the different mutants showed similar sizes and shapes, the number of inclusions per cell was variable (Fig. 1C). Approximately 60% of the cells expressing hSod1 A4V displayed inclusions, while around 20% of cells expressing other

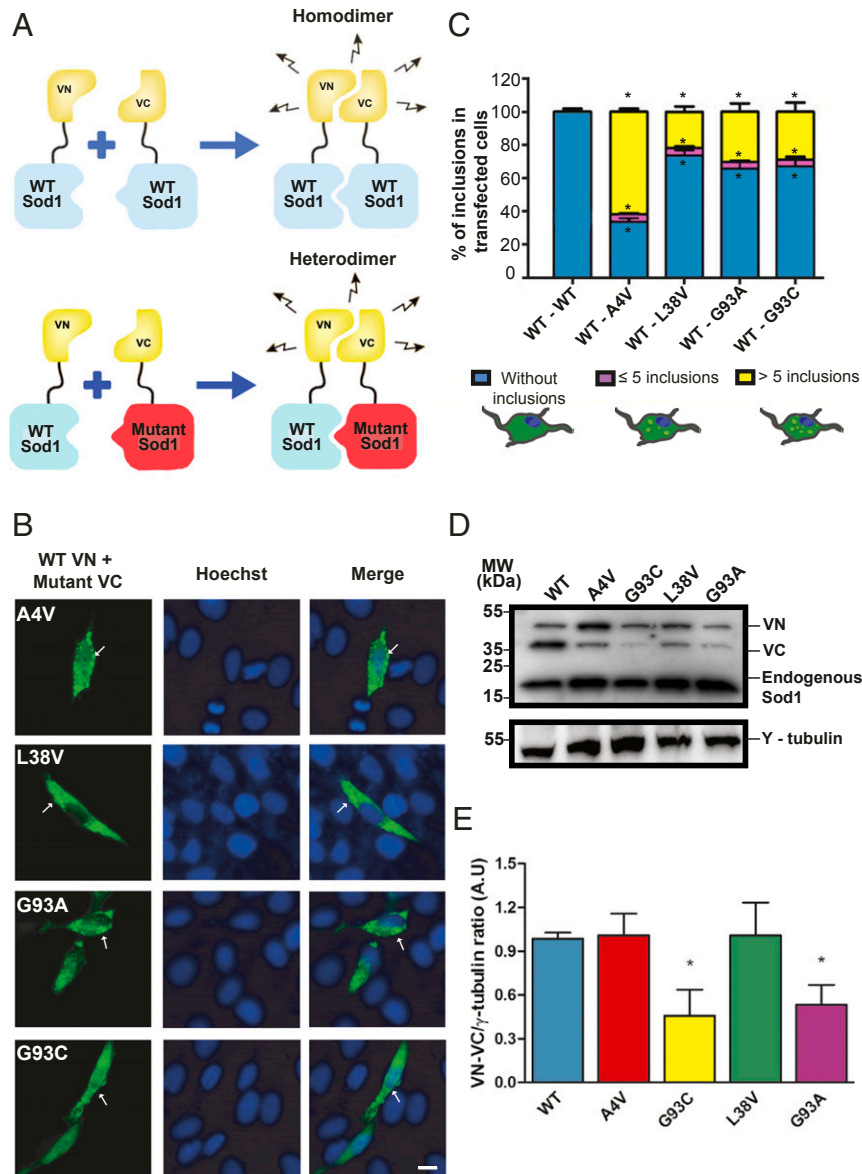


**Fig. 1.** Mutations affect Sod1 distribution and inclusion formation in human cell model. (A) Schematic representation of the BiFC assay. In the case of heterodimers, WT hSod1 was fused to C-terminal of VN fragment (VN-WT Sod1) and mutant hSod1 was tagged to N-terminal of VC fragment of Venus fluorescent protein (mutant Sod1-VC). To obtain WT hSod1 homodimers, cells contained WT Sod1-VC instead of mutant Sod1-VC. (B) Representative pictures of cells expressing fALS-related hSod1 mutant heterodimers. H4 cells expressing WT (VN-Sod1) and mutant hSod1 (Sod1-VC) (A4V, L38V, G93A, and G93C) were analyzed by fluorescence microscopy. Some hSod1 aggregates are pointed out by white arrows. (Scale bar: 10  $\mu$ m.) (C) Quantification of the number of inclusions per cell. At least 50 cells were counted per condition and classified in 3 different groups: blue, purple, and yellow bars represent the percentage of cells without any inclusion, with 5 or less inclusions and cells with more than 5 inclusions, respectively. Data were combined from at least 3 independent experiments. (D) Representative immunoblot confirming expression of VN-Sod1 and Sod1-VC fragments in H4 cells. (E) Quantification of the immunoblots. Data are expressed as mean  $\pm$  SD of at least 3 replicates. One-way ANOVA, with Bonferroni correction, was used for statistical analysis with significance level of  $*P < 0.05$ , which represents statistically different results between mutant hSod1 with the WT hSod1 variant (mutSod1 vs. WTSod1).

mutant hSod1 proteins displayed inclusions. In addition, the number of inclusions per cell was also different, with A4V forming more inclusions (>5 inclusions) than the other mutants. The levels of A4V and L38V mutants were identical, except those of G93A and G93C, suggesting these mutants may be more unstable in the cellular environment (Fig. 1 *D* and *E*).

**The A4V Mutation Affects the Intracellular Dynamics of hSod1.** Next, we assessed the dynamics of fALS-related Sod1 heteromeric inclusions using fluorescence recovery after photobleaching (FRAP). Prebleaching images were captured to estimate the initial fluorescence intensity, and the recovery after bleaching was analyzed (Fig. 2). We found that A4V inclusions exhibited the longest half-recovery time ( $24.91 \pm 4.90$ ), while inclusions formed by the other mutants exhibited similar values (L38V:  $4.71 \pm 1.00$ ; G93A:  $4.07 \pm 1.08$ ; G93C:  $5.26 \pm 1.80$ ) (Fig. 2*B*). This indicates that A4V inclusions are less labile than those formed by L38V, G93A, or G93C fALS variants.

**Sod1 WT–A4V Heterodimers Aggregate into Higher Molecular Weight Species.** The BiFC assay relies on the formation of, at least, protein dimers. However, given the nature of the assay, it does

not inform on whether nonfluorescent dimers may also accumulate in the same cells (e.g., dimers of Sod1–N-terminal region of Venus [VN] or of Sod1–C-terminal region of Venus [VC]). Thus, in order to investigate the types of species formed, we used human cells deficient (knocked down [KD]) in endogenous Sod1 (Sod1-KD), generated using CRISPR/Cas9 technology (SI Appendix, Figs. S1 and S2), and expressed the Sod1–VN and Sod1–VC constructs, as described above. Given the more robust findings with the WT–A4V pair, we focused on this mutant and performed immunocytochemistry (ICC) using antibodies against either Sod1 or an anti-GFP antibody that recognizes only the VC (SI Appendix, Fig. S3), in order to detect only 1 of the constructs. Using this approach, we distinguished the population of dimers formed by the complementation between VN and VC fragments (detected by the Venus signal), from either the total pool of Sod1 or from the pool of Sod1–VC (recognized by an anti-GFP antibody) (Fig. 3*A–C*). The overlap in BiFC signal with those detected upon immunostaining with either Sod1 or GFP antibodies confirmed that the majority of species formed by WT–WT (Fig. 3*A*), A4V–A4V (Fig. 3*B*), or WT–A4V (Fig. 3*C*) were detected by the BiFC assay, suggesting other types of dimers were absent, or were at least negligible.

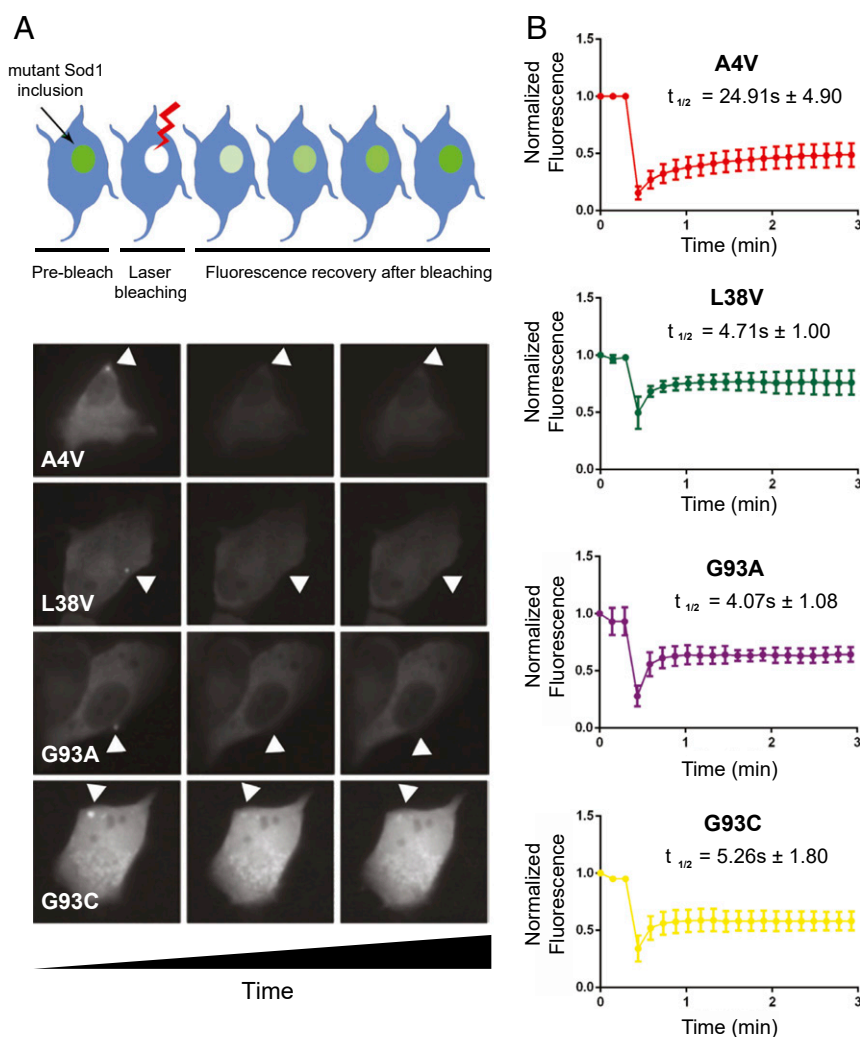


**Fig. 2.** Interaction dynamics of mutant Sod1 heterodimers in H4 cells. (*A*) In the *Upper* part, schematic illustration of FRAP of an inclusion of interest. At the *Bottom*, from left to right: a panel with 3 images of a representative cell expressing the heterodimer inclusion before photobleaching, just after photobleaching, and at the end of image acquisition. (*B*) FRAP recovery curves for heterodimers inclusions of VN–WT and mutant Sod1–VC. For each mutation, at least 6 inclusions in different cells were analyzed. Each plot represents mean  $\pm$  SD for each time point for all FRAP experiments.

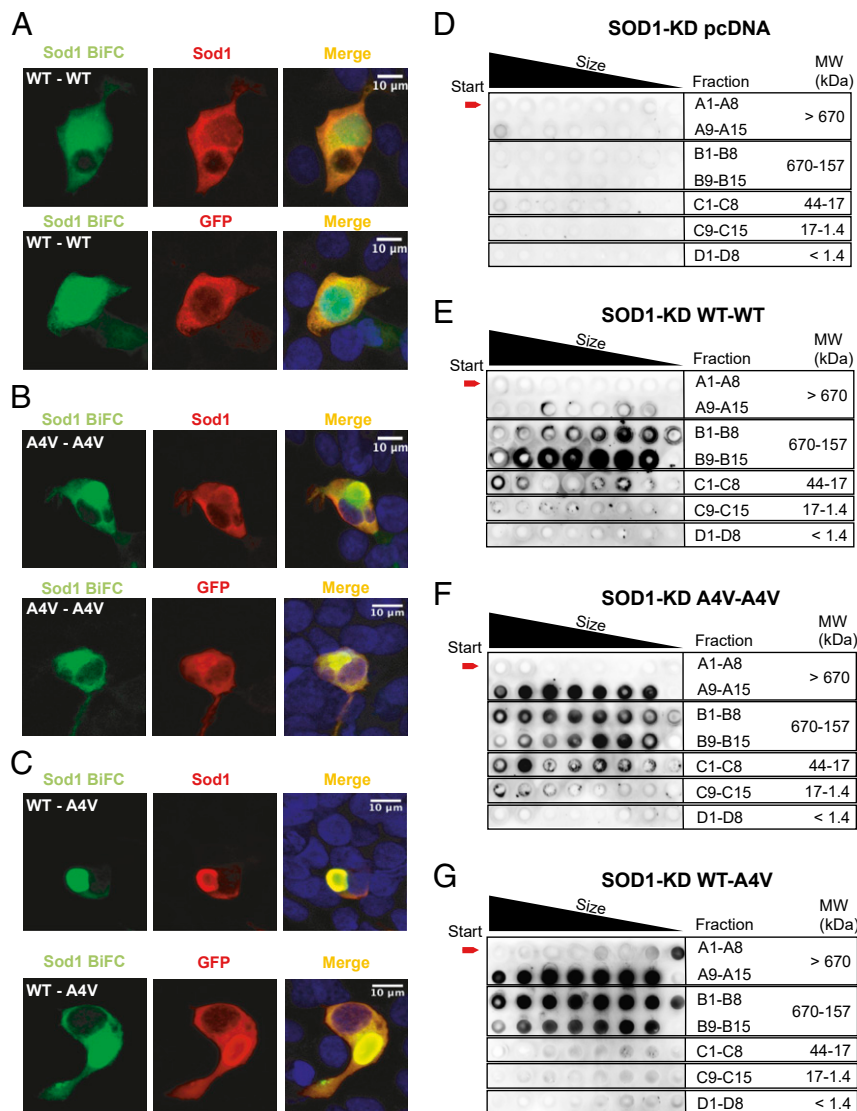


**Fig. 3.** hSod1 WT-A4V heterodimers aggregate into higher molecular weight species. HEK293 Sod1-KD cells were transfected with plasmids encoding the different hSod1 constructs (VN and VC fusions) and imaged using confocal microscopy (A–C). Each panel shows the fluorescence intensities of the BiFC signal counterstained with antibodies against Sod1 or GFP. The anti-GFP antibody used recognizes only the C-terminal fragment of Venus (VC). Sod1-KD cells expressing the homodimer hSod1-WT (A), the homodimer hSod1-A4V (B), and the heterodimer hSod1-WT-A4V (C). SEC followed by dot blot analysis using an anti-hSod1 antibody (D–G). SEC results are representative from at 3 independent experiments. Dot blot from Sod1-KD cells transfected with pcDNA3.1 (D), with WT-Sod1 BiFC constructs (E), with the A4V-Sod1 constructs (F), or with the WT-A4V-Sod1 constructs (G).

This finding is important as it demonstrates that the major population of dimers detected in the WT-A4V combination are, indeed, heterodimers.

Next, in order to compare the oligomerization state of hSod1, we separated total cell extracts using size-exclusion chromatography (SEC) (SI Appendix, Fig. S4) and assessed the presence of hSod1 in the fractions using dot blotting (Fig. 3D–G). Consistently with the microscopy results (Fig. 1), we found that WT-A4V hSod1 heteromers (Fig. 3G) formed higher molecular weight species than WT hSod1 homomers (Fig. 3E). We did not find inclusions in cells expressing WT hSod1 homomers (Fig. 1). Strikingly, WT-A4V heteromers formed even higher molecular weight species (Fig. 3G) than A4V homomers (Fig. 3F). Interestingly, we did not detect hSod1 in fractions C1–C8 (44 to 17 kDa), which might be expected to contain monomeric hSod1. This suggests that hSod1 heteromers, and not monomers, assemble into higher molecular weight species.

### Mutant hSod1 Heterodimers Display Reduced Dismutase Activity in Chronologically Aged Yeast Cells When Compared to Homodimers.

Yeast cells are ideally suited living test tubes for investigating the effect of oxidative stress on the molecular mechanisms associated with neurodegenerative diseases (18). Exponentially growing yeast cells obtain energy by fermentation and, consequently, produce low levels of reactive oxygen species (ROS), which increase in chronologically aged cells (18, 19). To investigate the functionality of the WT and mutant Sod1 heterodimers, we used *sod1Δ* yeast cells expressing WT or mutant hSod1-VN together with mutant hSod1-VC, to evaluate the effect of the hSod1 expression in the absence of endogenous yeast Sod1 (ySod1) activity. First, we confirmed the expression of hSod1 fused to either VN or VC fragments of Venus using an antibody against hSod1 (Fig. 4A), both before and after chronological aging. Next, we investigated the effect of chronological aging on mutant hSod1 activity. Aging, per se, did not alter WT hSod1 activity. However, *sod1Δ* cells expressing mutant A4V, G93A, or G93C homodimers, showed a



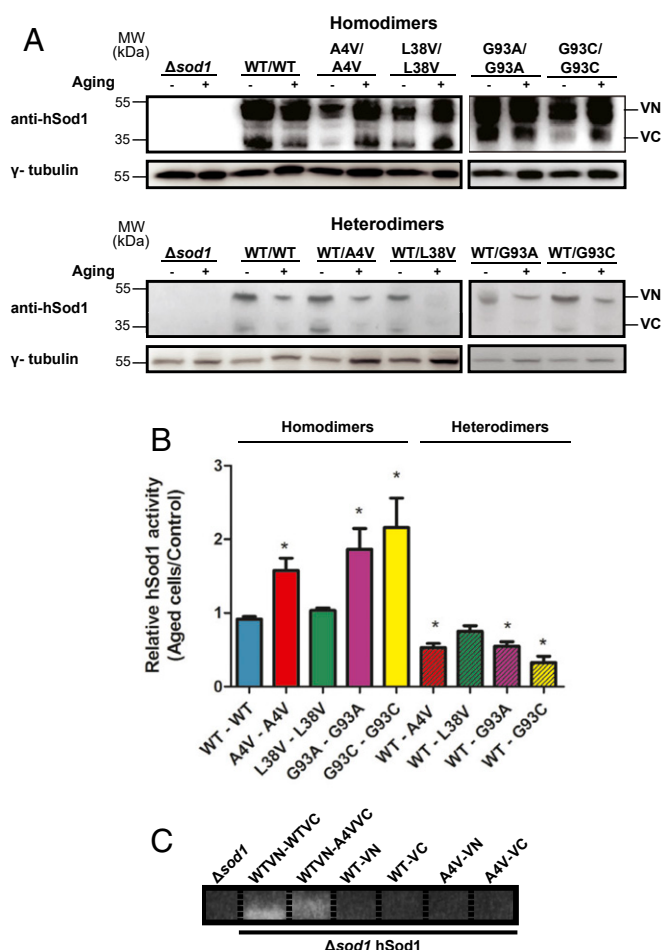


**Fig. 4.** Superoxide dismutase activity of hSod1 homo- and heterodimers. (A) Representative immunoblot confirming expression of VN-Sod1 and Sod1-VC fragments in yeast cells, both before and after aging conditions. (B) Superoxide dismutase activity was performed in exponential-phase *sod1Δ* cells expressing the hSod1, before and after chronological aging. Values are means  $\pm$  SD of at least 3 independent experiments and represent the ratio of hSod1 activity between aged and nonaged yeast cells. \* represents statistically different results between mutant hSod1 with the WT hSod1 variant (mutSod1 vs. WTSod1). Colored bars represent mutant homodimers, and hatched colored bars represent mutant heterodimers. (C) Sod1 activity of yeast *sod1Δ* cells expressing only the hSod1 VN or only presenting the VC fragment, in WT or A4V hSod1. Sod activity was performed in exponential-phase cells before chronological aging.

significant increase in dismutase activity upon aging (Fig. 4B). Interestingly, activity of A4V, G93A, or G93C mutant hSod1 heterodimers was decreased when compared with the homodimer counterparts and with WT Sod1 relative activity. Aging did not alter L38V Sod1 activity, neither homo- nor heterodimers.

To determine whether we were measuring only hSod1 activity of heterodimers, or if the homodimers (WT or A4V, as an example) were also present, we used yeast cells expressing Sod1 fused with only 1 of the fragments of Venus. Consistently with the observations in human cells, which showed no detectable hSod1 monomers or homodimers in cells expressing WT-A4V hSod1 (Fig. 3G), we found no hSod1 activity (i.e., dimerization) in cells expressing either VN- or VC-tagged hSod1 (Fig. 4C), suggesting, once again, that the dominant form of the hSod1 species formed upon coexpression of WT and mutant hSod1 was heteromeric/heterodimeric.

**hSod1 Heterodimers Are Not Able to Increase Longevity of *sod1Δ* Yeast Cells and to Protect Against Oxidative Damage.** To investigate whether the differences in activity between hSod1 homo- and heterodimers

affected yeast cells longevity, we determined the survival rates after chronological aging. We found that 44.9% of *sod1Δ* cells remained viable upon aging (Fig. 5). Overexpression of WT hSod1 in a *sod1Δ* background considerably increased the cellular viability to 90%, confirming the functional overlap between the yeast and human proteins. Strikingly, cells expressing WT-mutant Sod1 heterodimers displayed reduced viability when compared to cells expressing the individual homodimers, suggesting that the heterodimers are functionally impaired.

Aged cells show increased oxidative damage levels, which can be reversed by an effective antioxidant system. Consistent with this, expression of WT hSod1 in *sod1Δ* yeast reduced the damage caused by aging (Fig. 6). Confirming hSod1 heterodimer dysfunction, we found that cells expressing mutant hSod1 heterodimers displayed increased lipid peroxidation (Fig. 6A) and protein carbonylation (Fig. 6B). Surprisingly, expression of mutant hSod1 homodimers (A4V, L38V, and G93A) reduced the levels of lipid peroxidation upon aging. Expression of A4V or G93C hSod1 also reduced protein carbonylation. This suggests that different hSod1 mutants may influence the oxidative stress response in different ways, and that the toxicity associated with the formation of hSod1 heterodimers may be induced by oxidative modifications occurring in aged yeast cells.

**Aging Induces the Formation of hSod1 Inclusions in Yeast Cells.** Next, we investigated whether oxidative damage caused by chronological aging affected hSod1 aggregation in cells expressing homodimers or WT-mutant heterodimers. Exponentially growing *sod1Δ* cells expressing hSod1 homo- or heterodimers displayed no visible inclusions (Fig. 7A). In contrast, chronologically aged yeast cells expressing homo- or WT-mutant heterodimers accumulated

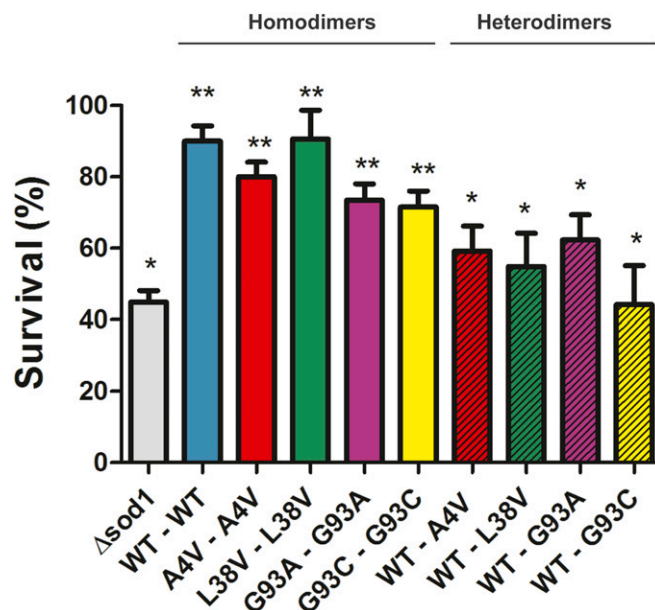


**Fig. 5.** Expression of WT-mutant heterodimers decreases cellular viability after 24 h aging. Yeast cell lacking endogenous Sod1 (*sod1Δ*) as well as carrying hSod1 (WT and mutants) were harvested at exponential phase and aged in water (nonproliferating condition) at 37 °C for 24 h. Cellular viability was carried out by counting plated cells on dropout 2% and expressed as the percentage of viable cells. Hatched and nonhatched colored bars represent mutant heterodimers and homodimers, respectively. The results represent the mean  $\pm$  SD of at least 3 independent experiments. \* represents statistically different results between *sod1Δ* or hSod1 mutants with the WT hSod1 variant (*sod1Δ* or mutants Sod1 vs. WT Sod1). \*\* statistically different results between recombinant yeast cells expressing hSod1 with the respective nonrecombinant strain, *sod1Δ* (WT or mutants hSod1 vs. *sod1Δ*).

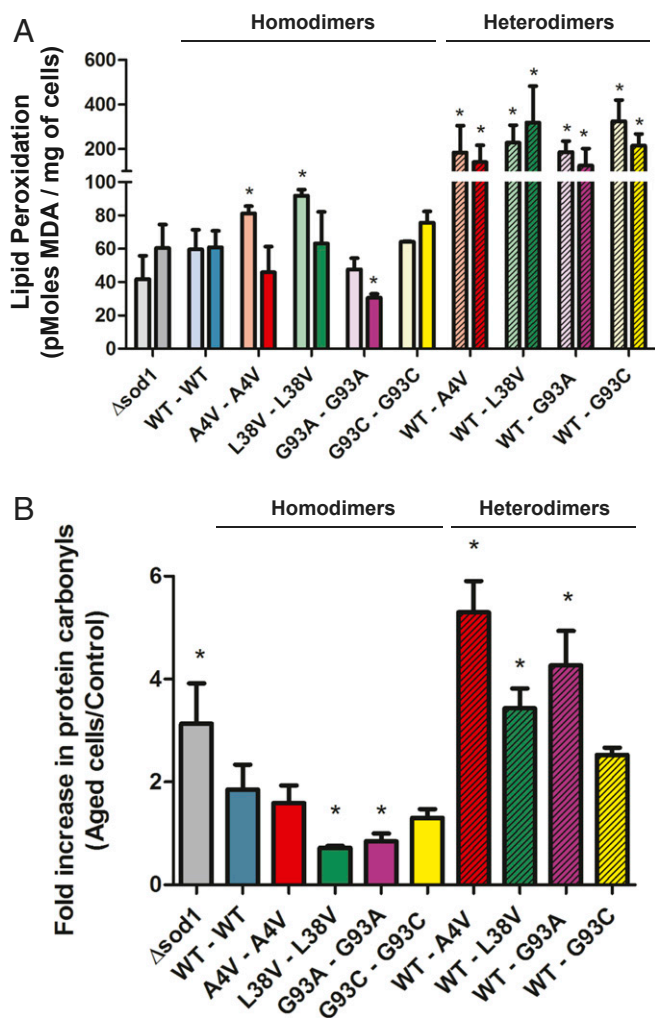


**Fig. 6.** The heterodimerization of WT and fALS mutant hSod1 significantly increases oxidative stress markers in chronologically aged yeast cells. Lipid peroxidation (A) and protein carbonylation (B) were determined in *sod1 $\Delta$*  recombinant cells expressing WT hSod1 or mutant homo- and heterodimers, before and after aging. Mutant heterodimers are represented by hatched bars on the Left side. (A) The lipid peroxidation levels were expressed in pMoles of MDA/mg of cells. As a control, the levels of MDA of nonaged cells (soft colored bars) of all recombinant strains and the nonrecombinant strain *sod1 $\Delta$*  were determined. The results carried out after aging are represented by dark colored bars. \* represents statistically different results between nonaged mutant homo- and heterodimers with the nonaged WT hSod1 variant (mutant Sod1 vs. WT hSod1), or aged mutants with aged hSod1WT. (B) Fold increase in protein carbonylation was measured as a ratio between protein carbonyl contents detected in aged yeast cells and the levels presented in nonaged yeast cells. The results represent the mean  $\pm$  SD of at least 3 independent experiments. \* represents statistically different results between mutant homo- or heterodimers with the WT hSod1 (*sod1 $\Delta$*  or mutant hSod1 vs. WT hSod1).

cytosolic inclusions, suggesting that oxidative stress increases the aggregation of fALS hSod1. We found that ~50% of aged yeast cells expressing hSod1 A4V homodimers displayed multiple inclusions, while the percentage of cells with inclusions was lower than 40% in cells expressing the other hSod1 mutants (Fig. 7B). Cells expressing WT and A4V, L38V, G93A, or G93C heterodimers displayed a larger number of inclusions per cell. Moreover, the percentage of cells with hSod1 inclusions significantly increased to ~80 in cells expressing WT-A4V heterodimers. In cells expressing the other homodimers or WT-mutant heterodimers, the percentage of cells with inclusions was between ~30% and ~50%.

As it can be seen in Fig. 8A, we found that WT hSod1 is localized in nucleus after the aging process. However, while ~80% of the cells expressing WT hSod1 showed hSod1 in the nucleus, the percentage of cells displaying nuclear localization of hSod1 dropped to less than 4% in cells expressing WT-mutant hSod1 heterodimers (Fig. 8B). To investigate whether the presence

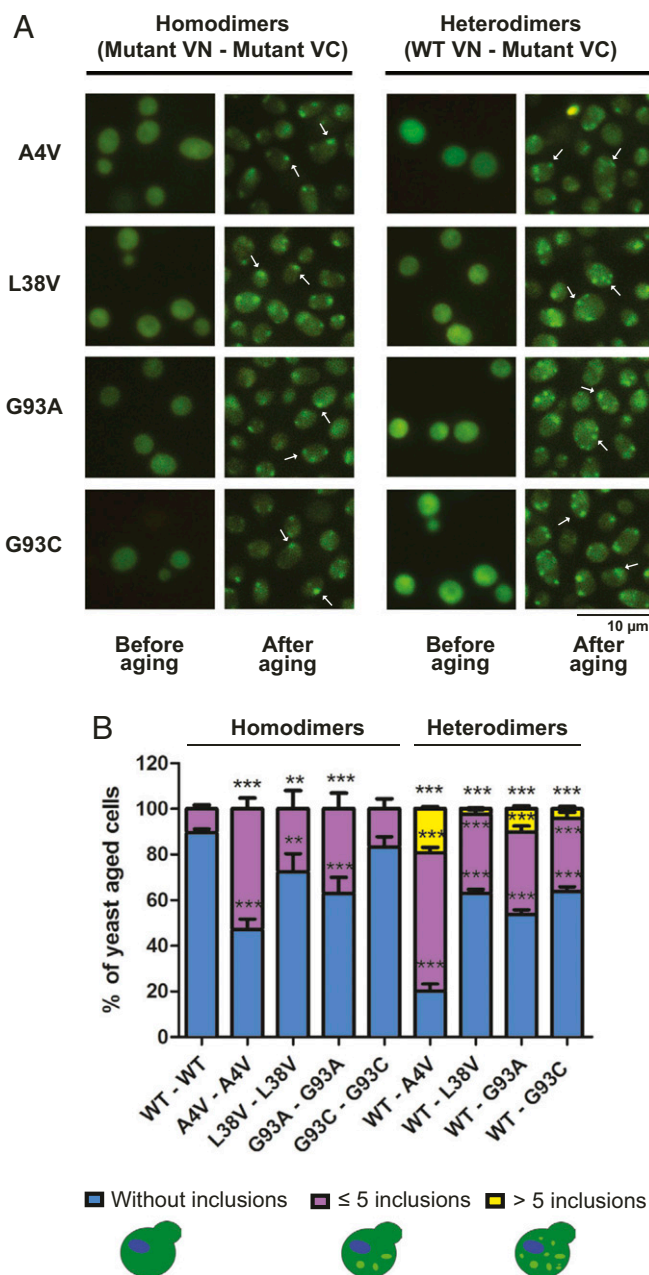


**Fig. 7.** Chronological aging induces the formation of mutant hSod1 cytoplasmic inclusions. (A) Representative pictures showing the localization of BiFC-hSod1 mutants in yeast cells imaged by fluorescence microscopy, both before and after aging. Arrows indicate some hSod1 inclusions. (Scale bar: 10  $\mu$ m.) (B) Quantification of the number of inclusions per cell. At least 50 cells were counted per condition and organized in 3 different categories which represent: the percentage of cells without any inclusion (blue bar), with 5 or less inclusions (purple bar), and yeast cells with more than 5 inclusions (yellow bars). One-way ANOVA, with Bonferroni correction, was used for statistical analysis with significance level of \*\*\* $P$  < 0.001 (WT vs. mutant cells). \*\* $P$  < 0.01 shows the significance level between WT and mutant cells. Data were combined from at least 3 independent experiments.

hSod1 in the nucleus is important to the antioxidant response, we measured catalase (Ctt1) activity in aged and dividing yeast cells. Ctt1 activity increased 3-fold after aging in the BY4741 control strain, expressing endogenous yeast Sod1 (Fig. 8C). The replacement of yeast Sod1 by WT hSod1 doubled Ctt1 activity in aged cells, suggesting that the nuclear hSod1 promoted the induction of genes involved in ROS resistance, including *CTT1*. In contrast, *sod1Δ* yeast cells expressing WT-mutant hSod1 heterodimers showed no or a lower increase in Ctt1 activity after aging when compared to *sod1Δ* WT hSod1. Taken together these results suggest that the cytosolic formation of WT-mutant hSod1 inclusions impairs the translocation of functional protein into the nucleus, compromising the antioxidant cell response and, consequently, cell longevity.

## Discussion

Here, we investigated the formation of heterodimers/heteromers between WT and ALS-associated mutant forms of hSod1 in living cells. The inclusions formed by the heteromeric combination demonstrated a higher propensity to aggregate into numerous inclusions per cell when compared to hSod1 mutant homodimers, as recently showed (9). The increased percentage of cells with WT-A4V heteromeric inclusions was consistent with the greater stability of the inclusions (assessed by FRAP) when compared to the other fALS Sod1 variants. Consistently with the accumulation of protein inclusions in cells, we found that WT-A4V hSod1 heteromers formed higher molecular weight species than A4V homomers, as confirmed by SEC analyses. Thus, we hypothesized that the inclusions formed by WT-mutant hSod1 heterodimers might be related to the toxicity of fALS-linked hSod1 mutants. In a previous study also using FRAP to investigate the inclusions formed by mutants of Fus, Tdp-43, or Sod1-GFP, it was found that the diffusion properties of Fus and Tdp-43 were significantly different from those formed by Sod1 A4V, which presented a rapidly

diffusing component (20). In that work, the authors expressed only the mutant form of hSod1. In contrast, FRAP measurements of Sod1 A4V heterodimers revealed very slowly diffusing species, which are consistent with stable inclusions.

By using differential immunostainings with anti-Sod1 and anti-GFP antibodies, we confirmed that the majority of oligomeric species formed in the cells could, indeed, be detected by the BiFC system, suggesting that cells coexpressing WT and A4V mutant hSod1 accumulate, primarily, heterodimers/heteromers. In *sod1Δ* yeast cells, the absence of hSod1 activity in cells expressing only VN or VC fusions, also confirmed that most hSod1 dimers formed in cells coexpressing VN and VC fusions resulted from the BiFC interaction, and that this may be sterically favorable, and perhaps stabilized by the assay.

Several studies in models of replicative or chronological aging suggest that the oxidative stress response is impaired and contributes to pathogenesis in fALS (9, 19, 21, 22). Regarding chronological aging, yeast and human cells, such as neurons, share several similarities (23–26). Given the remarkable advantages of yeast as a model for investigating the oxidative stress response of mutant hSod1, we took advantage of the BiFC system to study the activity and functionality of WT-mutant hSod1 heterodimers in chronologically aged yeast cells lacking the endogenous ySod1 (*sod1Δ*). We found that the activity of mutant hSod1 homodimers increased upon aging. On the other hand, the formation of dismutase-active mutant heterodimers was reduced in aged yeast cells. Although the fALS-associated hSod1 mutations studied here are considered to behave like the wild-type enzymes (27, 28), the oxidative stress induced by chronological aging modulates hSod1 activity, revealing a different but bona fide effect of the hSod1 mutant homo- and heterodimers in response to aging. Previously, it was suggested that dismutase-active WT hSod1 dimers might contribute to the toxicity caused by the presence of fALS-linked mutation (16). Indeed, the reduced hSod1 activity of mutant

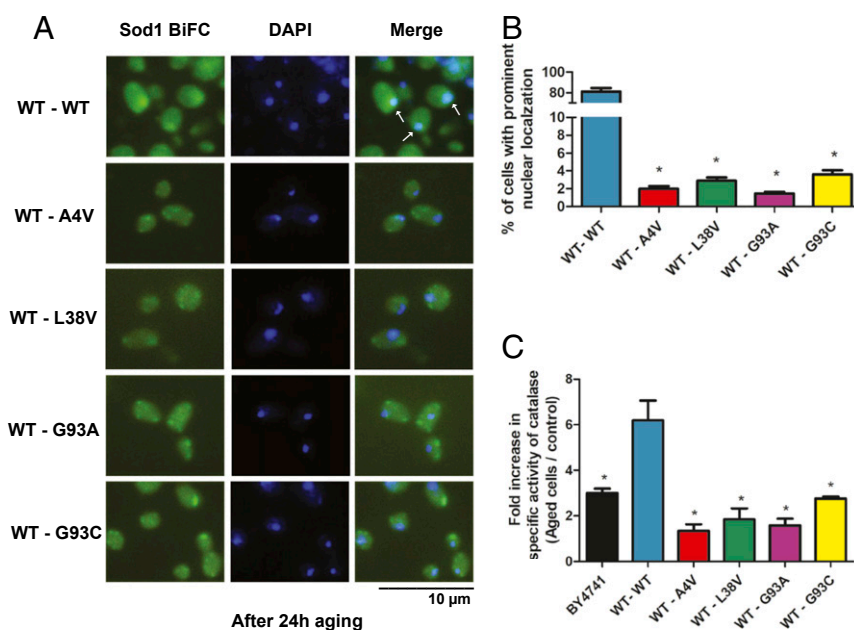


**Fig. 8.** hSod1 nuclear localization is impaired by fALS-linked mutations after aging. (A) hSod1 WT and mutant heterodimers were imaged by fluorescence microscopy after aging. Inclusions of Sod1 were visualized by expression of BiFC-tagged Sod1 (green), and the nucleus was stained by DAPI (blue). Arrows indicate the colocalization of the hSod1 with the nucleus, induced by the aging process. (Scale bar, 10  $\mu$ m.) (B) Percentage of cells with prominent Sod1 nuclear localization. Error bars indicate  $\pm$ SD of triplicates and at least 50 cells were counted per replicate. One asterisk represents statistically different results between mutant heterodimers with the WT hSod1 form (BY4741 or mutant hSod1 vs. WT hSod1). (C) Catalase activity results were expressed as a fold increase in specific activity (U/mg of protein) after chronological aging. One unit (U) of activity is defined as the amount of enzyme that catalyzes the consumption of 1  $\mu$ mol  $H_2O_2$ /min under the assay conditions. The results represent the mean  $\pm$  SD of at least 3 independent experiments. One-way ANOVA, with Bonferroni correction, was used for statistical analysis with significance level of  $*P < 0.05$  (WT vs. mutant cells or BY4741).



heterodimers correlated with the survival rates; cells expressing hSod1 heterodimers showed a decreased percentage of viable cells after chronological aging, compared to those expressing hSod1 WT. Otherwise, the highly active WT and mutant hSod1 homodimers increased lifespan considerably compared to *sod1Δ*, suggesting that mutant homodimerization provides benefits after 24 h aging. By contrast, the mutant heterodimers, but not homodimers, showed similar viability rates to the *sod1Δ* control cells. Neither the wild-type protein nor any of the currently modeled fALS mutations in yeast induced any severe growth defect (29–34). Thus, studies in chronologically aged *Saccharomyces cerevisiae* have successfully uncovered several aspects underlying the hSod1 activity as well as the cellular longevity upon the expression of hSod1 mutant (homo- and heterodimers) linked to fALS.

In vitro, the rates and free energy of heterodimerization ( $\Delta G_{\text{Het}}$ ) of ALS-associated mutant apo-Sod1 proteins (D90A, G37R, E100K, E100G, G93R, D101N, and N86D), suggest a possible correlation between the  $\Delta G_{\text{Het}}$  of each ALS Sod1 variant with patient survival time after diagnosis (35). The possible mechanisms of heterodimer formation were proposed to initiate from homodimeric forms, involving the swapping of subunits—the mutant and WT homodimers would first dissociate into monomers and then recombine into heterodimers or, alternatively, would initially associate into oligomers which would then dissociate into heterodimers (35). The proposed mechanisms did not consider that heterodimerization may also occur from recently new synthesized monomers (WT and mutant), which could interact and heterodimerize “de novo.” This de novo heterodimerization mechanism might also occur in our cell model and might be faster than the heterodimerization starting from homodimers.

In order to study homodimer association ( $k_a$ ) and dissociation ( $k_d$ ) constant rates from purified apo-Sod1 monomers, the experimental analyses were conducted under oxidizing conditions to keep the intramolecular disulfide linkage between C57 and C146 intact (36). WT and ALS mutants were produced on a background C6A/C111A (36), or C6A/C111S (37) in order to avoid artifacts from nonnative disulfide crosslinks (pseudo-Sod1 [pSod1]). The substitutions C6A/C111A, or C6A/C111S, were shown not to affect the stability or folding of Sod1 (36–39). The second-order  $k_a$  for WT or mutant pSod1 homodimer association is in the order of magnitude of  $10^7 \text{ M}^{-1} \text{ min}^{-1}$  while the constant rate of dissociation ( $k_d$ ) of the pSod1 homodimer dissociation and the constant rate of WT–ALS mutant heterodimerization ( $k_{\text{Het}}$ ) are around  $10^{-2} \text{ min}^{-1}$  (35–38). Although, there are no data for the constant rate for WT monomer–mutant monomer association, these analyses are consistent with the de novo heterodimerization mechanism, since this would be faster than starting from homodimer precursors.

Although the formation of homodimers is possible, the formation of functional homodimeric Sod1 was not detected in our system. This might be due to 2 possible explanations: 1) protein quality-control systems would primarily eliminate less stable proteins, consistently with studies reporting increased resistance against proteolytic degradation for mutant Sod1 heterodimers than for mutant Sod1 homodimers (16); and 2) steric hindrance of the fusion protein affecting mutant Sod1 homodimerization, which would have to be further investigated in independent studies.

We observed that the presence of all mutant heterodimers strongly increased lipid peroxidation. Furthermore, protein carbonylation dramatically raised after aging in WT–mutant hSod1 cells, especially for L38V, G93A, and A4V mutants. Our study establishes that the WT–mutant heterodimerization might actively contribute to enhance mutant hSod1 toxicity, resulting in cellular oxidative damages. Using high-resolution mass spectrometry (MS), high molecular weight (HMW) Sod1 species were found to be oxidized in residues critical for Sod1 activity (Cys146, His71, and His120) and stability. In addition, HMW  $P < 0.01$  Sod1–GFP

aggregation sharply increased in stationary-phase aged yeast cells, suggesting that oxidative damage may trigger Sod1 inclusion (40).

In order to investigate the effects of oxidative stress on hSod1 aggregation in aged yeast cells, we assessed aggregation and nuclear localization of WT and mutant hSod1 inclusions. We found that WT or mutant hSod1 did not form inclusions in young yeast cells harvested at midexponential phase. In contrast, mutant homo- and heterodimers form visible and multiple inclusions in chronologically aged cells. This was stronger for WT–A4V heteromers and suggested that the formation of mutant hSod1 aggregates might be directly related to oxidative damage caused by aging, affecting hSod1 dismutase activity and cellular viability. In response to elevated levels of ROS, WT hSod1 rapidly relocates into the nucleus, promoting the regulation of the oxidative stress resistance (5). Indeed, we confirmed that, during chronological aging, hSod1 relocates to the nucleus, efficiently stimulating cellular defense mechanisms against oxidative stress by the induction of genes involved in ROS resistance. Nevertheless, hSod1 mutants remain predominantly cytoplasmic, in inclusions, impairing the ROS-regulated change in cellular localization of hSod1. Indeed,  $\text{H}_2\text{O}_2$  was reported to be sufficient to promote Sod1 nuclear localization (5). Since catalase is one of the main antioxidant proteins involved in  $\text{H}_2\text{O}_2$  degradation and ROS resistance, we verified that Ctt1 activity is substantially higher in hSod1 WT-expressing cells after aging, when compared to that in cells expressing Sod1 heteromers.

A4V and G93A have been classified as class 1+2 mutations, which can destabilize the precursor monomers as well as weaken the dimer interface (8, 36). Interestingly, our data suggest the absence (or low levels) of monomeric species in Sod1-KD cells expressing WT–A4V heteromers, and the predominant formation of heteromeric, rather than homomeric species. Thus, on the basis of this result, we hypothesize WT hSod1 proteins may exist primarily as unfolded monomers and become fully active hSod1 dimers. On the other hand, mutant hSod1 proteins might exist primarily as unfolded/misfolded monomeric species (Fig. 9A). It has been shown that oligomer formation requires covalent disulfide bonds (C6–C111) between Sod1 monomers (38) that are much more stable than the dimerization interaction. In the presence of stable WT–mutant heterodimers, the formation of hSod1 heteromers seems to be initiated by Sod1 heterodimers due to the stability caused by the interaction with a WT folded monomer (Fig. 9B). Indeed, by observing an increase in resistance against proteolytic degradation, WT hSod1 stabilizes the folding of heterodimers compared to mutant homodimers (16). Hence, considering that WT hSod1 stabilizes mutant variants by heterodimerization as well as the inefficient heterodimer response against oxidative conditions, we hypothesize that mutant heterodimers may contribute to fALS-linked mutant hSod1 toxicity under aging conditions, opening avenues for the understanding

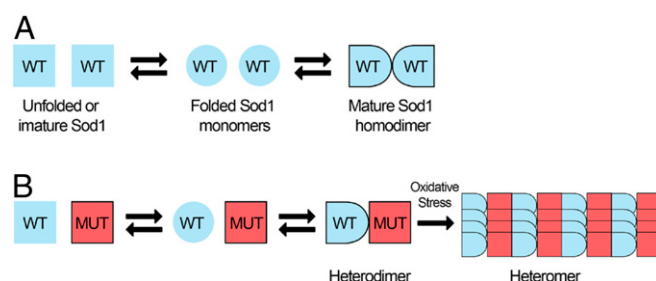


**Fig. 9.** Model for the formation and effects of WT–mutant hSod1 heteromers. (A) The folding and assembly of hSod1 WT into dimeric species. (B) The formation of Sod1 heteromers, which seems to be related to oxidative stress, possibly starts from hSod1 heterodimers species, and not from WT or mutant hSod1 monomers.



of the molecular mechanisms associated with mutant hSod1 toxicity.

## Materials and Methods

**Human Cell Culture and Transfections.** Human neuroglioma cells (H4) as well as human embryonic kidney 293 cells (HEK293) were cultured in Dulbecco's modified Eagle's medium (DMEM) (Life Technologies, Invitrogen), supplemented with 10% (vol/vol) fetal bovine serum (FBS) and 1% (vol/vol) penicillin-streptomycin, at 37 °C, and 5% CO<sub>2</sub> humidified atmosphere. Transfections in H4 cells were performed by the calcium phosphate method, and HEK293 cells were transfected, 24 h after plating, with Metafectene (Biontex Laboratories GmbH) according to the manufacturer's instructions. Equal amounts of plasmids encoding the WT or mutant (A4V, L38V, G93A, and G93C) hSod1 fused to the Venus-BiFC system were used for transfections. The cells were harvested 48 h posttransfection (9). WT hSOD1 cDNA was cloned to the 3' end of the VN fragment (VN-WT SOD1), while mutant hSOD1 cDNA was cloned upstream of the VC fragment (mutant SOD1-VC). The cDNA sequence of WT hSOD1 and hSOD1 mutants (coding for hSod1 A4V, L38V, G93A, or G93C) were subcloned from the yeast plasmid YEp351 into the Venus-BiFC plasmids, as previously described (9, 41).

**CRISPR/Cas9-Mediated Sod1-KD.** HEK293 cells were transiently transfected with the "all in one" vector PX459, expressing the guide RNA (gRNA) targeting 5'-GTGTGCGTCTGAAGGGCGCA-3' sequence in exon 1 of the hSOD1 gene using Metafectene according to the manufacturer's instructions. pSpCas9(BB)-2A-Puro (PX459) V2.0 (Addgene plasmid #62988; <http://www.addgene.org/62988/>; RRID:Addgene\_62988). After 48 h, cells were selected using 2 µg/mL puromycin (P11-0-19, PAA Laboratories) for 48 h. Cells were plated on 10-cm Petri dishes at a density of 1 cell/cm<sup>2</sup> and grown until they formed distinct colonies. Part of each colony was used to extract DNA, followed by sequencing of exon 1 of the SOD1 gene. Successfully edited colonies were further grown for subsequent experiments.

**Yeast Strains, Yeast Transformation, and Growth Conditions.** Human SOD1 cDNA (WT, A4V, L38V, G93A, and G93C) under the control of Sod1 promoter, were fused to the 3' end of the N-terminal (VN) or upstream of the C-terminal (VC) part of Venus (VN-SOD1, SOD1-VC) (42). These sequences were cloned into the *SacI* and *HindIII* sites of pRS425-pME2794 and pME2795 plasmids. The WT strain BY4741 (*MATa*; *his3*, *leu2*, *met15*; *ura3*) and its isogenic mutant *sod1Δ* (*SOD1::KanMX4*), were acquired from Euroscarf. Stocks of all strains were maintained on solid dropout 2% medium (2% glucose, 0.67% yeast nitrogen base without amino acids, 0.2% of dropout mixture, 2% agar). For all experiments, cells were grown up to midexponential phase (~1 mg dry weight/mL) in liquid dropout 2% medium with or without leucine and uracil, at 28 °C and 160 rpm, with the ratio/flask volume medium of 5:1. While for homodimers construction yeast cells were transformed using pME2794 plasmid (VN) and pME2795 (VC), containing either 1 copy of WT-VC and WT-VN or mutant human SOD1-VC and mutant human SOD1-VN, to construct heterodimers, yeast cells were transformed using the same plasmids, but containing WT-VN and mutant human SOD1-VC. Transformation of the cells was performed by electroporation method (43) and then selected by plating on solid dropout 2% medium without leucine and uracil.

**BiFC Plasmids.** As previously described (9, 44), the Venus-BiFC plasmids were subcloned with the cDNA sequence of human WT SOD1 and the mutants A4V, L38V, G93A, and G93C. This cDNA sequence was obtained from the yeast plasmid YEp351.

**Quantification of hSod1 Inclusions.** After transfection (48 h), Dulbecco's PBS (DPBS) was used to wash H4 cells. Then, the cells were fixed with 4% paraformaldehyde (PFA) for 10 min at room temperature (RT), and washed 3 times with DPBS. For fluorescence microscopy, H4 cells were stained with Hoechst 33258 (Life Technologies, Invitrogen) (1:5,000 in DPBS) for 5 min. A Leica DMI 6000B microscope was used for fluorescence images acquisition (9).

For yeast cell analysis, an aliquot of yeast culture (1 mL of suspension 1 mg/mL) was centrifuged and resuspended in 200 µL of distilled water. A total of 1 µL of this suspension, added with 1 µL of n-propyl gallate and 1 µL of 4'-6-diamino-2-phenylindole (DAPI) (1:10,000 vol/vol) (Sigma-Aldrich), was added in a slide and maintained in dark for fluorescence microscopy. Fluorescence images were acquired with an Olympus IX73 microscope. For each result, at least 50 transfected cells per strain and condition were detected, scored based on hSod1 inclusions pattern, and classified into 3 groups: cells without inclusions, 5 or less inclusions (≤5 inclusions), and more than 5 inclusions (>5 inclusions) (9, 44).

**FRAP.** FRAP experiments were performed in H4 cells using a Leica 6000B microscope equipped with a large incubator maintained at 37 °C, 5% CO<sub>2</sub>. Images were acquired at intervals of 10 s. In each FRAP experiment, hSod1 inclusions were bleached using a 488-nm laser line at 100% laser transmission on a circular region of interest. Images were acquired using Metamorph software (Omicron Laserage) and image processing as well as fluorescence intensity measurements performed by using ImageJ software (42, 45).

**Immunocytochemistry.** Immunocytochemistry was performed according to Guerreiro et al. (46). H4 cells were washed with PBS and fixed with paraformaldehyde solution 4% in PBS, 48 h posttransfection. The solution containing PBS 0.1% Triton X-100 was used to permeabilize the cells, followed by a blocking step for 1 h with 1.5% BSA and an overnight incubation of the primary antibody for anti-Sod1 (Santa Cruz Biotechnology), 1:1,000, and anti-GFP (B-2, Santa Cruz Biotechnology), 1:1,000. After 3 washes with PBS, the secondary antibody anti-goat or anti-mouse IgG conjugated to Alexa Fluor 555 (A31570, Invitrogen, Thermo Fisher Scientific) 1:1,000 was incubated at RT for 1 h. DAPI staining (6355.1, Roth; 0.5 µg/mL) was used to assess the cell nuclei. Fluorescent confocal images were captured using a Leica Microsystems microscope (Leica SP5).

**Fractionation of Total Protein Extracts by SEC and Dot Blot.** As previously described (46), 48 h posttransfection, Sod1-KD cells were harvested by centrifugation (10 min at 5 °C and 10,000 × g) in a phosphate buffer (TBS with 0.5% Triton X-100) containing protease inhibitor mixture (Roche). By using a 0.45-µm Spin-X centrifuge filter (Sigma), 1.5 mg of total protein in a final volume of 500 µL was filtered, and subsequently loaded on a Superose 6 (10/300 GL, GE Healthcare Life Science) column. After this, a HPLC (HPLC) (Åkta Purifier10, GE Healthcare Life Science) was performed in ammonium acetate buffer (50 mM, pH 7.4) with a flow rate of 0.5 mL/min. SEC fractions of 500 µL were collected, boiled at 95 °C for 10 min, and centrifuged at 14,000 × g, 5 °C for 5 min. Then, the collected fractions were probed for hSod1 using immunodot assay.

**Immunoblotting.** Total protein extracts were obtained from 48-h transfected H4 cells, by lysis with radioimmunoprecipitation assay (RIPA) buffer, and fractionated in 15% SDS/PAGE, as described before (9). The same protocol was also followed for the running and transference of the gels, which, thereafter, were incubated with primary antibody 1:2,000 anti-hSod1 and mouse 1:5,000 anti-γ-tubulin overnight at 4 °C. Then, membranes were incubated for 1 h with anti-goat IgG and anti-mouse secondary antibodies conjugated to horseradish peroxidase at 1:6,000.

Yeast protein extracts were also fractionated by SDS/PAGE, using 15% polyacrylamide gels as described (19). The same protocol was also followed for the running and transference of the gels. The membranes were incubated for 2 h with a rabbit anti-hSod1 and further for 2 h with anti-rabbit IgG conjugated to horseradish peroxidase. Detection was carried out using luminol reagent and peroxide solution (Millipore). The band intensity was estimated using ImageJ software.

**Chronological Aging of Yeast Cells.** Midexponential phase yeast cells were centrifuged at 2,500 × g for 5 min and washed twice with distilled water. Cell pellets were resuspended in water and incubated at 37 °C, 160 rpm, during 24 h (19). Aged cells were harvested, and the experiments performed accordingly.

**Evaluation of Yeast Longevity and Oxidative Damage.** Cell viability before and after chronological aging was analyzed by plating in triplicate on solidified dropout 2% medium after proper dilution. The plates had been incubated at 28 °C for 72 h, and the colonies were counted. Viability was determined before and after growth (47–49). Malondialdehyde, a final product of lipid peroxidation, was measured by thiobarbituric acid reactive species (TBARS) method (50). Protein carbonylation, used as a biomarker of protein oxidation, was assayed by slot blot by using a primary anti-DNP (dinitrophenyl) (D9656, Sigma-Aldrich Merck) followed by incubation with a secondary antibody anti-rabbit IgG conjugated with peroxidase (A0545, Sigma-Aldrich Merck) (19, 51).

**Superoxide Dismutase and Catalase Activity.** Extracts for enzymatic determinations were obtained by the disruption of yeast cells (50 mg) with 1.5 g of glass beads in 50 mM sodium phosphate buffer pH 7.8, containing a protease inhibitor mixture (cOmplete, mini, EDTA-free protease mixture inhibitor tablets; Sigma-Aldrich Merck). Protein concentration was determined according to Stickland (52) using BSA as standard. Sod1 activity was measured in situ after native polyacrylamide gel electrophoresis from 80 µg of protein in the presence of riboflavin and nitroblue tetrazolium (NBT). The activity was determined

based on the ability of superoxide dismutase to inhibit the reduction of NBT by superoxide radical (19). Then, polyacrylamide gel electrophoresis was digitalized on the EC3 imaging system (UVP Bioimaging Systems), and Sod1 bands were analyzed, taking into consideration the area density by the use of ImageJ software. Catalase activity was determined by measuring H<sub>2</sub>O<sub>2</sub> consumption at 240 nm (53).

**Statistical Analyses.** Data were analyzed using GraphPad Prism 5 software and expressed as mean values  $\pm$  SD of at least 3 independent experiments. Statistical differences were calculated using 1-way and 2-way ANOVA with Bonferroni correction. Significance was assessed: \**P* < 0.05, \*\**P* < 0.01, and \*\*\**P* < 0.001.

**Data Availability.** All data generated or analyzed during this study are included in this published article and its supplementary information files.

**ACKNOWLEDGMENTS.** This work was supported by Higher Education Improvement Coordination (CAPES), National Council for Scientific and Technological Development (CNPq), and Foundation for Research Support of the State of Rio de Janeiro (FAPERJ). T.F.O. was supported by the German Research Foundation (DFG) Center for Nanoscale Microscopy and Molecular Physiology of the Brain. We thank MSc. José Raphael Monteiro and Prof. Dr. Cristian Follmer from Laboratory of Biological Chemistry of Neurodegenerative Diseases (Federal University of Rio de Janeiro) for technical assistance.

1. R. Sirabella *et al.*, Ionic homeostasis maintenance in ALS: Focus on new therapeutic targets. *Front. Neurosci.* **12**, 510 (2018).
2. M. Katsuno, F. Tanaka, G. Sobue, Perspectives on molecular targeted therapies and clinical trials for neurodegenerative diseases. *J. Neurol. Neurosurg. Psychiatry* **83**, 329–335 (2012).
3. D. Majoor-Krakauer, P. J. Willems, A. Hofman, Genetic epidemiology of amyotrophic lateral sclerosis. *Clin. Genet.* **63**, 83–101 (2003).
4. R. A. Saccon, R. K. A. Bunton-Stasyshyn, E. M. C. Fisher, P. Fratta, Is SOD1 loss of function involved in amyotrophic lateral sclerosis? *Brain* **136**, 2342–2358 (2013).
5. C. K. Tsang, Y. Liu, J. Thomas, Y. Zhang, X. F. S. Zheng, Superoxide dismutase 1 acts as a nuclear transcription factor to regulate oxidative stress resistance. *Nat. Commun.* **5**, 3446 (2014).
6. H. Deng *et al.*, Amyotrophic lateral sclerosis and structural defects in Cu,Zn superoxide dismutase. *Science* **261**, 1047–1051 (1993).
7. D. R. Rosen *et al.*, Mutations in Cu/Zn superoxide dismutase gene are associated with familial amyotrophic lateral sclerosis. *Nature* **362**, 59–62 (1993).
8. J. Kim *et al.*, Dimerization, oligomerization, and aggregation of human amyotrophic lateral sclerosis copper/zinc superoxide dismutase 1 protein mutant forms in live cells. *J. Biol. Chem.* **289**, 15094–15103 (2014).
9. A. A. Brasil *et al.*, Implications of fALS mutations on Sod1 function and oligomerization in cell models. *Mol. Neurobiol.* **55**, 5269–5281 (2018).
10. L. Wang *et al.*, Wild-type SOD1 overexpression accelerates disease onset of a G85R SOD1 mouse. *Hum. Mol. Genet.* **18**, 1642–1651 (2009).
11. D. Jaarsma *et al.*, Human Cu/Zn superoxide dismutase (SOD1) overexpression in mice causes mitochondrial vacuolization, axonal degeneration, and premature motoneuron death and accelerates motoneuron disease in mice expressing a familial amyotrophic lateral sclerosis mutant SOD1. *Neurobiol. Dis.* **7**, 623–643 (2000).
12. H.-X. Deng *et al.*, Conversion to the amyotrophic lateral sclerosis phenotype is associated with intermolecular linked insoluble aggregates of SOD1 in mitochondria. *Proc. Natl. Acad. Sci. U.S.A.* **103**, 7142–7147 (2006).
13. T. E. Brotherton, Y. Li, J. D. Glass, Cellular toxicity of mutant SOD1 protein is linked to an easily soluble, non-aggregated form in vitro. *Neurobiol. Dis.* **49**, 49–56 (2013).
14. M. Prudencio, A. Durazo, J. P. Whitelegge, D. R. Borchelt, Modulation of mutant superoxide dismutase 1 aggregation by co-expression of wild-type enzyme. *J. Neurochem.* **108**, 1009–1018 (2009).
15. H. Witan *et al.*, Wild-type Cu/Zn superoxide dismutase (SOD1) does not facilitate, but impedes the formation of protein aggregates of amyotrophic lateral sclerosis causing mutant SOD1. *Neurobiol. Dis.* **36**, 331–342 (2009).
16. A. Weichert *et al.*, Wild-type Cu/Zn superoxide dismutase stabilizes mutant variants by heterodimerization. *Neurobiol. Dis.* **62**, 479–488 (2014).
17. S. A. Gonçalves, J. E. Matos, T. F. Outeiro, Zooming into protein oligomerization in neurodegeneration using BiFC. *Trends Biochem. Sci.* **35**, 643–651 (2010).
18. A. V. Oliveira, R. Vilaça, C. N. Santos, V. Costa, R. Menezes, Exploring the power of yeast to model aging and age-related neurodegenerative disorders. *Biogerontology* **18**, 3–34 (2017).
19. A. A. Brasil *et al.*, The involvement of GSH in the activation of human Sod1 linked to fALS in chronologically aged yeast cells. *FEMS Yeast Res.* **13**, 433–440 (2013).
20. N. E. Farrarwell *et al.*, Distinct partitioning of ALS associated TDP-43, FUS and SOD1 mutants into cellular inclusions. *Sci. Rep.* **5**, 13416 (2015).
21. G. H. Kim, J. E. Kim, S. J. Rhie, S. Yoon, The role of oxidative stress in neurodegenerative diseases. *Exp. Neurobiol.* **24**, 325–340 (2015).
22. M. Peled-Kamar *et al.*, Oxidative stress mediates impairment of muscle function in transgenic mice with elevated level of wild-type Cu/Zn superoxide dismutase. *Proc. Natl. Acad. Sci. U.S.A.* **94**, 3883–3887 (1997).
23. V. D. Longo, G. S. Shadel, M. Kaerberlein, B. Kennedy, Replicative and chronological aging in *Saccharomyces cerevisiae*. *Cell Metab.* **16**, 18–31 (2012).
24. V. D. Longo, P. Fabrizio, Chronological aging in *Saccharomyces cerevisiae*. *Subcell. Biochem.* **57**, 101–121 (2012).
25. M. Kaerberlein, Lessons on longevity from budding yeast. *Nature* **464**, 513–519 (2010).
26. A. Arlia-Ciommo, A. Piano, A. Leonov, V. Svistkova, V. I. Titorenko, Quasi-programmed aging of budding yeast: A trade-off between programmed processes of cell proliferation, differentiation, stress response, survival and death defines yeast lifespan. *Cell Cycle* **13**, 3336–3349 (2014).
27. J. A. Rodriguez *et al.*, Familial amyotrophic lateral sclerosis-associated mutations decrease the thermal stability of distinctly metallated species of human copper/zinc superoxide dismutase. *J. Biol. Chem.* **277**, 15932–15937 (2002).
28. L. J. Hayward *et al.*, Decreased metallation and activity in subsets of mutant superoxide dismutases associated with familial amyotrophic lateral sclerosis. *J. Biol. Chem.* **277**, 15923–15931 (2002).
29. C. R. Nishida, E. B. Gralla, J. S. Valentine, Characterization of three yeast copper-zinc superoxide dismutase mutants analogous to those coded for in familial amyotrophic lateral sclerosis. *Proc. Natl. Acad. Sci. U.S.A.* **91**, 9906–9910 (1994).
30. L. B. Corson, J. J. Strain, V. C. Culotta, D. W. Cleveland, Chaperone-facilitated copper binding is a property common to several classes of familial amyotrophic lateral sclerosis-linked superoxide dismutase mutants. *Proc. Natl. Acad. Sci. U.S.A.* **95**, 6361–6366 (1998).
31. M. A. Hough *et al.*, Dimer destabilization in superoxide dismutase may result in disease-causing properties: Structures of motor neuron disease mutants. *Proc. Natl. Acad. Sci. U.S.A.* **101**, 5976–5981 (2004).
32. E. L. Bastow, C. W. Gourlay, M. F. Tuite, Using yeast models to probe the molecular basis of amyotrophic lateral sclerosis. *Biochem. Soc. Trans.* **39**, 1482–1487 (2011).
33. E. L. Bastow *et al.*, New links between SOD1 and metabolic dysfunction from a yeast model of Amyotrophic Lateral Sclerosis (ALS). *J. Cell Sci.* **129**, 4118–4129 (2016).
34. S. Rabizadeh *et al.*, Mutations associated with amyotrophic lateral sclerosis convert superoxide dismutase from an antiapoptotic gene to a proapoptotic gene: Studies in yeast and neural cells. *Proc. Natl. Acad. Sci. U.S.A.* **92**, 3024–3028 (1995).
35. Y. Shi, M. J. Acerson, A. Abdolvahabi, R. A. Mowery, B. F. Shaw, Gibbs energy of superoxide dismutase heterodimerization accounts for variable survival in amyotrophic lateral sclerosis. *J. Am. Chem. Soc.* **138**, 5351–5362 (2016).
36. M. J. Lindberg, R. Byström, N. Boknäs, P. M. Andersen, M. Oliveberg, Systematically perturbed folding patterns of amyotrophic lateral sclerosis (ALS)-associated SOD1 mutants. *Proc. Natl. Acad. Sci. U.S.A.* **102**, 9754–9759 (2005).
37. A.-K. E. Svensson *et al.*, Metal-free ALS variants of dimeric human Cu,Zn-superoxide dismutase have enhanced populations of monomeric species. *PLoS One* **5**, e10064 (2010).
38. M. J. Lindberg, J. Normark, A. Holmgren, M. Oliveberg, Folding of human superoxide dismutase: Disulfide reduction prevents dimerization and produces marginally stable monomers. *Proc. Natl. Acad. Sci. U.S.A.* **101**, 15893–15898 (2004).
39. L. Banci, I. Bertini, C. Y. Chiu, G. T. Mullenbach, M. S. Viezzoli, Synthesis and characterization of a monomeric mutant Cu/Zn superoxide dismutase with partially reconstituted enzymic activity. *Eur. J. Biochem.* **234**, 855–860 (1995).
40. D. Martins, A. M. English, SOD1 oxidation and formation of soluble aggregates in yeast: Relevance to sporadic ALS development. *Redox Biol.* **2**, 632–639 (2014).
41. T. F. Outeiro *et al.*, Formation of toxic oligomeric  $\alpha$ -synuclein species in living cells. *PLoS One* **3**, e1867 (2008).
42. S. Tenreiro *et al.*, Yeast reveals similar molecular mechanisms underlying alpha- and beta-synuclein toxicity. *Hum. Mol. Genet.* **25**, 275–290 (2016).
43. J. R. Thompson, E. Register, J. Curotto, M. Kurtz, R. Kelly, An improved protocol for the preparation of yeast cells for transformation by electroporation. *Yeast* **14**, 565–571 (1998).
44. D. F. Lázaro *et al.*, Systematic comparison of the effects of alpha-synuclein mutations on its oligomerization and aggregation. *PLoS Genet.* **10**, e1004741 (2014).
45. S. Tenreiro *et al.*, Phosphorylation modulates clearance of alpha-synuclein inclusions in a yeast model of Parkinson's disease. *PLoS Genet.* **10**, e1004302 (2014).
46. P. S. Guerreiro *et al.*, LRRK2 promotes tau accumulation, aggregation and release. *Mol. Neurobiol.* **53**, 3124–3135 (2016).
47. M. D. C. de Carvalho, J. F. De Mesquita, E. C. A. Eleutherio, In vivo characterization of I91T Sod2 polymorphism of *Saccharomyces cerevisiae*. *J. Cell. Biochem.* **118**, 1078–1086 (2017).
48. F. A. Castro, D. Mariani, A. D. Panek, E. C. Eleutherio, M. D. Pereira, Cytotoxicity mechanism of two naphthoquinones (menadione and plumbagin) in *Saccharomyces cerevisiae*. *PLoS One* **3**, e3999 (2008).
49. E. T. V. Trevisol, A. D. Panek, S. C. Mannarino, E. C. A. Eleutherio, The effect of trehalose on the fermentation performance of aged cells of *Saccharomyces cerevisiae*. *Appl. Microbiol. Biotechnol.* **90**, 697–704 (2011).
50. E. L. Steels, R. P. Learmonth, K. Watson, Stress tolerance and membrane lipid unsaturation in *Saccharomyces cerevisiae* grown aerobically or anaerobically. *Microbiology* **140**, 569–576 (1994).
51. P. D. B. Adamis *et al.*, Lap4, a vacuolar aminopeptidase I, is involved in cadmium-glutathione metabolism. *Biometals* **22**, 243–249 (2009).
52. L. H. Stickland, The determination of small quantities of bacteria by means of the biuret reaction. *J. Gen. Microbiol.* **5**, 698–703 (1951).
53. G. Rona *et al.*, CTT1 overexpression increases life span of calorie-restricted *Saccharomyces cerevisiae* deficient in Sod1. *Biogerontology* **16**, 343–351 (2015).